The Properties of Transparent Film Made from Linear Polyethylene by Irradiation Cross-Linking

R. Kitamaru,* H.-D. Chu, and S.-H. Hyon

Institute for Chemical Research, Kyoto University, Uji, Kyoto, 611, Japan.
Received July 28, 1972

ABSTRACT: Highly transparent films were made from linear polyethylene by irradiation cross-linking. The thermodynamic properties as well as the crystalline structure of the films were studied. It was confirmed that the transparent films have very high melting temperatures and a highly ordered and stable crystalline phase, but a rather low degree of crystallinity. X-Ray studies revealed that the samples have a very special spatial orientation of the crystalline phase. *C* axes are located almost perfectly parallel to the film plane, and crystal planes (110) and (200) are oriented preferentially parallel to that plane. The origin of the transparency is discussed with respect to this spatial orientation of the crystalline phase.

A number of papers have appeared recently[1-7] describing procedures for preparing transparent polyethylene of high crystallinity. Southern and Porter[1] obtained a transparent polyethylene strand by crystallization of the flowing melt of the polymer in a capillary rheometer under very high pressure and shear (the capillary-flowing procedure). Wang, Kwei, and Chen[4] developed a procedure for preparing transparent film by dropping molten polyethylene between two rotating polished rollers that were kept at room temperature and were kept in contact with each other with high pressure (the quenched-roll procedure). It was also reported that a transparent filament could be obtained by plastic flow of the polymer either in a capillary[6] or in tapered dies[7] under very high pressure. The properties of the various transparent products, of course, were different but the products exhibited some common characteristics, such as high moduli or high melting temperatures together with high transparency. This suggests similar crystalline structures that resulted from similar modes of crystallization.

During "capillary-flowing," or "quenched-rolling," or "plastic-flowing" procedures, transparent products are obtained by either crystallization or recrystallization under conditions of high molecular orientation. To attain such structures, rather severe conditions such as very high pressure and shear are thought to be necessary. However, if high molecular orientation during the crystallization is sufficient to obtain transparent products, any other procedures of crystallization that involve high degrees of molecular orientation would result in a similar product in the absence of high pressure and shear.

A lightly cross-linked polyethylene of adequate cross-link density can be elastically deformed in the molten state until molecular chains are almost fully extended.[8] If the lightly cross-linked polyethylene is crystallized from such a deformed state by cooling to room temperature, the crystallization of oriented molecular chains will be achieved in the absence of high pressure and shear. We have studied this mode of crystallization and found conditions that give transparent films[9,10] or filaments.[11] The structure and properties of these films have been reported briefly.[9-12] This paper concerns this crystallization method for preparing transparent films and describes the film properties in detail.

Preparation of Samples

Three kinds of lightly cross-linked samples of linear polyethylene were used in this study. The starting material for the first was a molecular weight fraction from Hostalen (commercial high-density polyethylene from Hoechst) with a viscosity average molecular weight of 3.4×10^6. The viscosity average molecular weight was obtained from intrinsic viscosity measurements in decalin at 135° using the relation $[\eta] = 6.2 \times 10^{-4} M^{0.70}$ established by Chiang.[13] The unfractionated whole Hostalen polymer was used for the second sample. It had a viscosity average molecular weight of 2.5×10^6. The last polymer used as starting material was commercial Marlex 50 with a viscosity average molecular weight of 136×10^3. It was used without any molecular weight fractionation. Films about 1.5-mm thick were first irradiated to different dosages in vacuum using different sources of high energy ionizing radiation. After irradiation, the gel fraction w_g (mass fraction of the nonsoluble part to the total mass) was evaluated by extracting with boiling xylene and drying. The irradiation conditions and the gel fractions of the resultant products are listed in Table I.

Note that only 0.25 Mrad gave a w_g of 0.97 for the very high molecular weight fraction while a dose of 22.5 Mrad resulted in a w_g of 0.77 for the commercial Marlex 50 whole polymer of medium molecular weight. The cross-link density and the concentration of the free end groups, *i.e.*, molar fraction of units cross-linked and that of the end groups in the entire system, respectively, were estimated for the samples from the gel point and the molecular weight before irradiation using the theory of gel formation of linear polymers.[14,15] For the gel from sample I, the cross-link density and the concentration of the free end groups were found to be 1.6×10^{-5} and 7.4×10^{-6}, respectively. These quantities were not determined for the irradiated products of samples II and III, but were supposed to be appreciably larger than those for the gel from

(1) J. H. Southern and R. S. Porter, *J. Macromol. Sci., Phys.*, **4**, 541 (1970).
(2) J. H. Southern and R. S. Porter, *J. Appl. Polym. Sci.*, **41**, 2305 (1970).
(3) C. R. Desper, J. H. Southern, R. D. Ulrich, and R. S. Porter, *J. Appl. Polym. Sci.*, **41**, 4284 (1970).
(4) T. T. Wang, H. S. Chen, and T. K. Kwei, *J. Polym. Sci., Part B*, **8**, 505 (1970).
(5) T. K. Kwei, T. T. Wang, and H. E. Bair, *J. Polym. Sci., Part C*, **31**, 87 (1970).
(6) R. G. Crystal and J. H. Southern, *J. Polym. Sci., Part A-2*, **9**, 1641 (1971).
(7) K. Imada, T. Yamamoto, K. Shigematsu, and M. Takayanagi, *J. Materials Sci.*, **6**, 537 (1970).
(8) R. Kitamaru and H.-D. Chu, *Bull. Inst. Chem. Res., Kyoto Univ.*, **46**, 97 (1968).
(9) H.-D. Chu and R. Kitamaru, *Kobunshi Kagaku*, **29**, 214 (1972).
(10) R. Kitamaru, H.-D. Chu, and W. Tsuji, *Polym. Prepr., Amer. Chem. Soc., Div. Polym. Chem.*, **13**, 298 (1972).
(11) R. Kitamaru, S.-H. Hyon, and C. Tsuchiya, 47th Annual Meeting of the Society of Fiber Science and Technology, Tokyo, May, 1972.
(12) R. Kitamaru, *Chem. Tech.*, in press.
(13) R. Chiang, *J. Polym. Sci.*, **36**, 91 (1959).
(14) W. H. Stockmayer, *J. Chem. Phys.*, **12**, 125 (1944).
(15) P. J. Flory, *J. Amer. Chem. Soc.*, **69**, 30 (1947).

Table I
Starting Materials and Irradiation Procedures

Starting Material	1. Mol Wt Fraction from Hostalen, $\bar{M}\eta = 3.4 \times 10^6$	2. Commercial Whole Polymer, Hostalen (Hoechst), $\bar{M}\eta = 2.5 \times 10^6$	3. Commercial Whole Polymer, Marlex 50, $\bar{M}\eta = 0.136 \times 10^6$
Radiation			
Beam	X-Ray from van de Graaff	Electron from van de Graaff	γ Ray, ^{60}CO
Dosage (Mrad)	0.25	2.7	22.5
Irradiated *in vacuo*	At 150°	At room temperature	At room temperature
The gel fraction after irradiation, W_g	0.97	0.90	0.77

Table II
Melting Temperature, Density, and Transparency of Films Made from the Cross-Linked Polyethylene Listed in Table I with Different Compression Ratios

	Compression Ratio	Density	Melting Temp (°C)	Transparency[c]
Sample I	1:10	0.942	155.0	+++
Sample II	1:1[a]	0.935	137.6	
	1:1[b]	0.932	136.8	
	1:6.7	0.9370	151.5	++
	1:8	0.9378	153.2	+++
	1:10	0.9380	155.0	+++
Sample III	1:1[a]	0.950	137.5	
	1:1[b]	0.935	130.7	
	1:2.9	0.937	129.8	
	1:4.3	0.938	129.7	+
	1:6.5	0.939	130.5	++
	1:7.5	0.940	135.0	+++
	1:9.1	0.940	133.5	+++
	1:10.5	0.941	136.5	+++
	1:14	0.944	136.7	+++

[a] Well crystallized. [b] Quenched from the melt by 15 min. [c] Transparency: + = good, ++ = very good, +++ = excellent.

sample I, because of the smaller molecular weight and the larger irradiation dose for these samples than for sample I.

All of the lightly cross-linked samples displayed rubbery elasticity in the molten state and could be stretched uniaxially more than tenfold. However, there was some residual strain after stress was released. The original length was recovered by swelling at high temperature with a solvent of linear polyethylene and then drying. The three lightly cross-linked films were compressed to different extents between two polished metal plates at 160–180° and cooled to room temperature over a period of 15 min. The cross-linked film from sample I was used after extracting its soluble fraction, but those from samples II and III were used without removing those soluble fractions. In this procedure, the film thicknesses were reduced and the properties as well as transparency of the products were improved progressively according to the extent of the compression. Table II summarizes the relationship between the compression ratio and the density or melting temperature for the three samples. The compression ratio is here defined to be the ratio of the film thickness after compression to the original thickness. The density was determined at 30° with a toluene–dioxane density gradient column and the melting temperature was measured by differential scanning calorimetry with a heating rate of 10°/min as described in the following section.

As can be seen, excellent transparency was obtained when the compression ratios were less than 1:6 to 1:7. Extraordinarily high melting temperatures such as 155° were observed for samples from the two higher molecular weight polymers (fractionated and unfractionated samples). But similar high melting temperatures were not obtained for samples from Marlex 50 of ordinary molecular weight. In the following sections, transparent films made from the three samples by high compression with compression ratios less than 1:8 will be discussed.

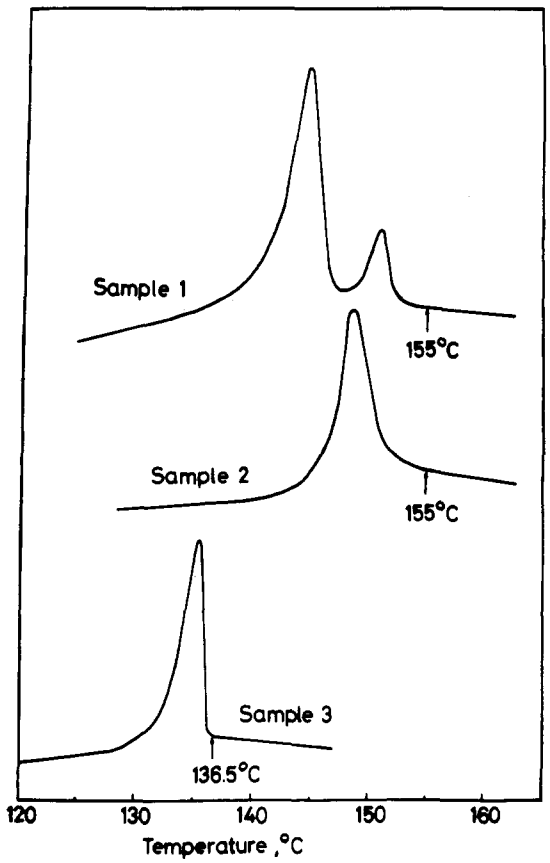

Figure 1. DSC fusion scan for the transparent films made from cross-linked polyethylene listed in Table I. Compression ratio 1:10. Rate of scan 10°/min.

Fusion and Melting Temperature

The fusion behavior of samples was studied with a Perkin-Elmer DSC 1-B. Figure 1 shows the DSC fusion curves for a heating rate of 10°/min for the transparent films made from the three cross-linked samples listed in Table I. Melting temperatures increased with decreasing compression ratios for each sample as shown in Table II, but this section only concerns samples made using a compression ratio of 1:10. Characteristic dual peaks are observed in the fusion of sample I. In addition to a peak at temperatures corresponding to normal fusion for isotropically well-crystallized linear polyethylene, another isolated sharp peak appears at a temperature much higher than the normal melting point of polyethylene. Although sample II has only one peak, the temperature level at which it

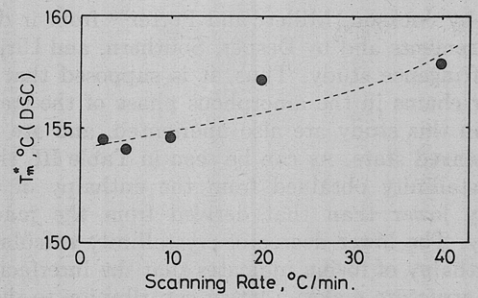

Figure 2. Melting temperature *vs.* scan rate for sample I listed in Table I (compression ratio 1:10).

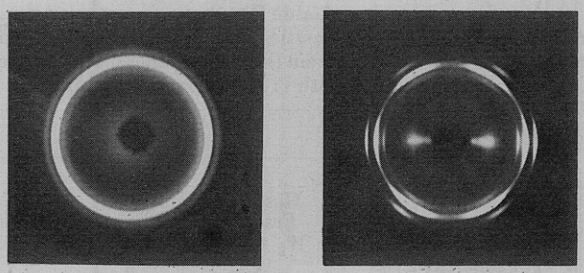

Figure 3. X-Ray wide-angle diffraction patterns for sample I listed in Table I (compression ratio 1:10): A, through view; B, edge view; film edge; vertical.

appears is as high as that of the second peak of sample I. The melting temperature was 155° for both samples I and II. The melting temperature was defined as the point at which the fusion curve returned to the base line after completion of fusion.

Sample III had the rather low melting temperature of 136.5° as might be expected from its high cross-link density and large concentration of free end groups caused by both the larger irradiation dosage of 22.5 Mrad and the limited molecular weight of the starting material. If the cross-link density is large, it will result in both a lower crystallinity and an increased number of macromolecular chains that are insensitive to macroscopic deformation. However, the melting temperature of III is exceptionally high, since isotropic quenching of the sample from the melt to room temperature over a period of 15 min gave a melting point of 130.7° (see line 8 of Table II).

The 155° melting temperature for samples I and II was not only much higher than those reported for transparent polyethylene strand or film made by other procedures,[2,5] but it also was rather independent of the heating rate of the DSC scan. It has been reported that the melting temperature of transparent strands made by the capillary-flowing procedure, decreased with decreasing scan rate, ultimately reaching 137–138°, the extrapolated value at zero scan rate.[2] On the other hand a similar plot for sample I in Figure 2 shows that the extrapolated melting temperature is still about 154°. Melting temperatures higher than those for normally well-crystallized polyethylene were sometimes observed in DSC scans of stress-induced solution crystals of linear polyethylene.[16-18] Such phenomena are generally thought to be attributable to superheating effects during scanning of crystals from oriented molecular chains.[18] The very high melting temperature for samples I and II may be due to similar superheating effects.

When a DSC scan was made with a sample held at constant length, Clough[19] obtained a dual fusion curve very similar to that of sample I for a uniaxially stretched polyethylene gel. The melting temperature was 152° for his sample with a very low cross-link density. The high melting temperature could be expected from a decrease in enthalpy of fusion, if the sample length was kept constant during fusion. Although the film dimensions of our sample were not held constant during the DSC scan, the sample behaved as though they were constant. For example, sample I exhibited a dual fusion peak and samples I and II had very high melting temperatures that were independent of the scan rate. As mentioned in the first section the minor strain remaining in our samples could only be removed by swelling with a linear polyethylene solvent at high temperatures. Therefore, the characteristic melting behavior of our samples must result from a structural anisotropy remaining even after completion of fusion.

Unit-Cell Density and Crystallinity

The radiograph was taken with a 114.6-mm powder camera, with manganese-filtered Fe Kα radiation, and with the film fixed asymmetrically. A number of d spacings of the crystal planes of the orthorhombic crystalline form of the samples were determined. The errors due to film shrinkage and to radius deviation of the camera were corrected using forward and backward diffractions of samples containing NaF.[20] Other systematic errors caused by factors, such as miscentering of samples in the camera, were corrected by the use of a plot of the lattice parameter of NaF against $\cos^2\theta$ according to the method of Bradby and Jay,[21] where θ is the Bragg angle for different crystal planes of NaF. Thus, the a-axis dimension was determined from d spacings for crystal plane (400) and the d spacing pairs for (210) and (020), (310) and (020), and (310) and (110), respectively. The b-axis dimension was determined from the d spacing for (020) and a pair of d spacings for (310) and (110). The different calculation procedures yielded values that were in close agreement for both a and b lattice parameters. The average values of the cell dimensions were used for further studies. Furthermore the c axis in sample II was determined from the cell-dimensions a and b together with any one of the d spacings determined for (111), (201), or (211). The average value of the c axis was 2.547 ± 0.0005 Å. However, the c dimension of samples I and II could not be obtained experimentally, because the diffractions from crystal planes (111), (201), and (211) were too faint to read, probably due to a highly crystalline orientation for the former and to imperfections in the crystalline phase of the latter sample.

The unit-cell density was obtained from the cell parameters a, b, and c, using the relation $d_u = 4M_0/abcN$. Here, M_0 is the molecular weight of the methylene unit and N is Avogadro's number. With atomic weight c = 12.011, H = 1.0080, and $N = 6.023 \times 10^{23}$, the equation reduces to $d_u = 93.153/abc$, where the unit-cell dimensions are in Angstrom units. All a-, b-, and c-axis dimensions were experimentally obtained for sample II as described above. The c axis for samples I and III was assumed to be 2.547 Å, the value obtained for sample II. The results are summarized in Table III together with the macroscopic density and the degree of crystallinity at 30°. The degree of crystallinity was calculated either from the

(16) B. Wunderlich, C. M. Cormier, A. Keller, and M. J. Machin, *J. Macromol. Sci., Phys.*, 1, 93 (1967).
(17) T. W. Huseby and H. E. Bair, *J. Polym. Sci., Part B*, 5, 265 (1967).
(18) A. M. Rijke and L. Mandelkern, *J. Polym. Sci., Part A-2*, 8, 225 (1970).
(19) S. B. Clough, *J. Appl. Polym. Sci.*, 15, 214 (1971).
(20) R. Kitamaru and L. Mandelkern, *J. Polym. Sci., Part A-2*, 8, 2079 (1970).
(21) H. P. Klug and L. E. Alexander, "X-ray Diffraction Procedures," John Wiley & Sons, Inc., New York, N. Y., 1954, p 461.

Table III
Macroscopic, Unit-Cell Densities, and Other Thermodynamic Properties of Films Made from the Cross-Linked Polyethylene Listed in Table I with 1:10 Compression Ratio

Properties	Sample I Hostalen, Fraction $W_g = 0.97$, Gel	Sample II Hostalen, Whole $W_g = 0.90$	Sample III Marlex 50, Whole $W_g = 0.77$
Macroscopic density	0.942	0.938	0.941
Melting temperature (°C)	155.0	155.0	136.5
Degree of crystallinity[a]			
$(1 - \lambda)_d$	0.65	0.62	0.64
$(1 - \lambda)_{\Delta H}$	0.560	0.566	0.570
Lattice parameters			
a	7.392	7.398	7.427
b	4.939	4.943	4.954
c		2.547	
Unit-cell density	1.002[b]	1.000	0.994[b]

[a] $(1 - \lambda)_d$, calculated from densities at 30°, $(1 - \lambda)_{\Delta H}$, calculated from the enthalpy of fusion. [b] Assumed $c = 2.547$.

macroscopic density assuming additivity in densities of the crystalline and amorphous phases or from the enthalpy of fusion divided by 70 cal/g (the enthalpy of fusion for a perfect crystal of polyethylene).

First, it is noted that the lattice parameters a and b observed in this study are very small values, and the unit-cell densities are either equal to or larger than unity for samples I and II. Particularly, the unit-cell density of sample I (1.002) is the largest value reported for linear polyethylene to date.[20,22-27] Such a highly stable crystalline phase also should be expected from the extraordinarily high melting temperature of 155.0° observed for the samples. A slightly smaller unit-cell density is observed for sample III. However, the macroscopic densities and, therefore, the calculated degrees of crystallinity of all samples are rather low contrary to expectations based on the high melting temperatures and high unit-cell densities. A higher melting temperature or a larger unit-cell density for an isotropically well-crystallized polyethylene are generally associated with a larger macroscopic density and, therefore a higher degree of crystallinity. The converse is observed for samples in this study and is attributed to a stable crystalline phase. It must be concluded that the samples contain a very stable but smaller crystalline fraction coexisting with a rather large amorphous fraction.

At this moment, no information about the amorphous phase in these samples is available, but some is available for the uniaxially stretched and crystallized cross-linked sample. Birefringence studies by Chu, Kitamaru, and Tsuji[28] showed that in a lightly cross-linked polyethylene, prepared by high stretching in the molten state and subsequent cooling, a very highly uniaxially oriented crystalline phase coexisted with a large amorphous fraction having a low orientation. A low degree of orientation of molecules in the amorphous phase of a transparent strand prepared by the capillary-flowing procedure was also proposed by Jackson, Miller, and Porter[29] from ir dichroism measurements and by Desper, Southern, and Ulrich[3] from a birefringence study. Thus, it is supposed that the molecular chains in the amorphous phase of the transparent films in this study are also unoriented, and are probably in a relaxed state. As can be seen in Table III, the degree of crystallinity obtained from the enthalpy of fusion is slightly lower than that derived from the macroscopic density. The lower degree of crystallinity calculated from the enthalpy of fusion indicates that the interfacial region in the structure makes a larger contribution to the enthalpy of fusion than to the macroscopic density as discussed by Mandelkern, Allou, and Gopalan.[30] However, the difference between the degrees of crystallinity calculated from the density and from the enthalpy of fusion is smaller for all samples studied here than for that reported for normally crystallized polyethylene.[30] This may imply that the structure of the interfacial region in these samples is rather simple and that molecular chains in the amorphous phase are in a relaxed state. This is in accord with the conclusion reached above from the birefringence and ir dichroism data for the uniaxially stretched cross-linked sample or for the transparent strand made by the capillary-flowing procedure.

The Mechanical Properties

Some mechanical properties of sample I with a compression ratio of 1:8 are listed in Table IV, together with data of a normally compression-molded film of uncross-linked polymer. Although a minor orientation dependence was observed for the properties of sample I, only average values representing different orientations are listed in the table. The dynamic modulus was measured with a Vibron DD2 instrument operating at 110 cps at 25°; the static tensile properties were measured with a Tensilon apparatus obtained from the Toyo Measuring Instrument Co.; and the Young's Modulus and strength at break are based on the specimen cross-section at zero stress. The shrinking temperature is the point at which samples begin to contract in air and the per cent shrinkage values were measured in air at a heating rate of 1°/min.

The dynamic and Young's moduli and the strength at break are higher and the elongation is lower for sample I than the corresponding values for the normally compression-molded film. The high moduli for the sample are in good accord with the data for the transparent strand[2] and film[5] made by other procedures. This may imply the presence of a crystalline structure similar to that in those samples. In any case, the mechanical properties and resistance to thermal deformation are excellent. Heat shrinkage only occurs above 120° and is only 12.5% and 60% at 130 and 150°, respectively. This excellent dimensional stability can be attributed either to the highly ordered and stable crystalline structure or to the relaxed state of the amorphous phase in the sample. Also, relaxed amorphous material should provide excellent low temperature properties.

The Orientation of Crystallites

Figure 3 shows the wide-angle X-ray diffraction patterns for sample I with a compression ratio of 1:10. The patterns were taken by a flat camera using Ni-filtered Cu $K\alpha$ radiation with the beam introduced either perpendicular (through view) or parallel (edge view) to the sample film. These photographs not only indicate the very high

(22) C. Bunn, *Trans. Faraday Soc.*, **35**, 482 (1939).
(23) E. R. Walter, F. P. Reding, *J. Polym. Sci.*, **21**, 561 (1956).
(24) P. R. Swan, *J. Polym. Sci.*, **42**, 525 (1960); *ibid.*, **56**, 403 (1962).
(25) M. I. Bank and S. Krimm, *J. Appl. Phys.*, **39**, 4951 (1968).
(26) G. T. Davis, R. K. Eby, and G. M. Martin, *J. Appl. Phys.*, **39**, 4973 (1968).
(27) S. Kavesh and J. M. Schultz, *J. Polym. Sci., Part A-2*, **8**, 243 (1970).
(28) H.-D. Chu, R. Kitamaru, and W. Tsuji, *J. Appl. Polym. Sci.*, **10**, 1377 (1966).
(29) J. F. Jackson, P. J. Miller, and R. S. Porter, *Polym. Prepr., Amer. Chem. Soc., Div. Polym. Chem.*, **13**, 335 (1972).
(30) L. Mandelkern, A. L. Allou, Jr., and M. Gopalan, *J. Phys. Chem.*, **72**, 309 (1968).

Table IV
Mechanical Properties of a Transparent Film

Sample	Dynamic[a] Modulus (dyn/cm²)	Young's Modulus (kg/cm²)	Strength at Break (kg/cm²)	Elongation at Break (%)	Shrinking Temp (°C)	Shrinking % at 120°	130°	150°
I[b]	2.27×10^{10}	1.87×10^{4}	1.02×10^{3}	84	120	0	12.5	60
Reference[c]	1.84×10^{10}	1.35×10^{4}	2.96×10^{2}	1100	75	17.5		

[a] Measured on a Vibron DD2 at 110 cps at 25°. [b] Sample I in Table I, compression ratio 1:8. [c] A normally compressed and annealed film of the starting fraction of sample I.

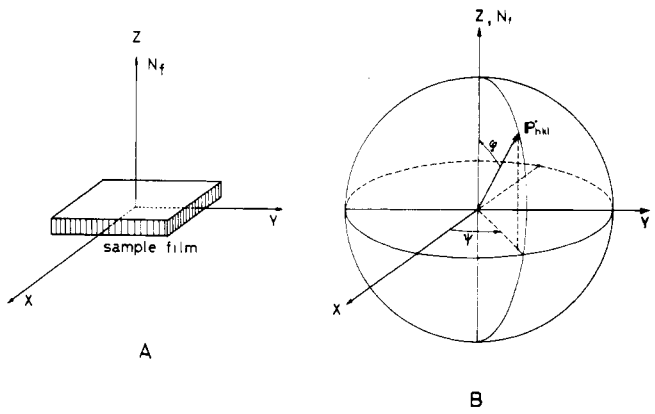

Figure 4. Geometry of spatial distribution for a crystal plane P* in the samples.

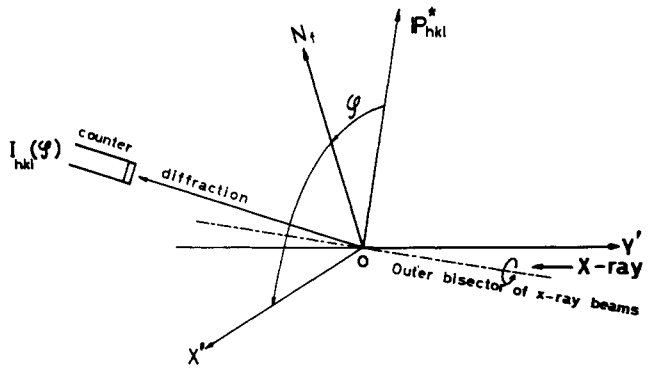

Figure 5. Geometry for an X-ray scan.

crystalline content of the sample but also indicate a special spatial orientation of the crystalline phase. It can be concluded, however, from the uniform circular distribution in the pattern (through view), that crystallites are randomly oriented about the normal to the film surface (uniaxially oriented around the normal to the film surface). This uniaxial orientation was confirmed for most parts of the sample by X-ray patterns. If crystallites are located randomly with respect to the normal to the sample film, the spatial distribution of each crystal plane in the sample could be defined solely as a function of angle between two normals to the film and to a crystal plane. The geometry for this is shown in Figure 4. Here, vector $\mathbf{P}^*_{hkl}$ represents a crystal plane (hkl) in the reciprocal crystal lattice and the sample is fixed in the coordinate system (x, y, z), the z axis of which coincides with the film normal N_f. Thus, the distribution function Φ_{hkl} for each $\mathbf{P}^*_{hkl}$ in the sample can be expressed as a function of φ. In order to evaluate this distribution function $\Phi(\varphi)$ for different crystal planes, a detailed X-ray scan was made for parts of samples I and III with a compression ratio of 1:10, in which an uniaxial crystallite orientation around N_f was indicated by the flat camera X-ray diffraction photographs such as the through view in Figure 3. To do this, diffraction intensity was recorded by a proportional counter against the rotating angle of N_f. In this scan the counter was set at an angle 2θ against the incident beam and the samples were rotated so that N_f was rotated around the outer bisector of the indicent beam to the sample and diffractive beam to the counter, starting from the position of the inner bisector of the beams to 90° (see Figure 5). Since the diffraction intensity $I(\varphi)$ was recorded as a function of rotating angle φ, it should be proportional to the distribution function $\Phi(\varphi)$ for the crystal plane.

Thus, scans for (110), (200), (210), (020), and (011) were performed for the two samples. The results for (011) are shown in Figure 6. We note that no appreciable intensity was recorded for sample I in the range of $\varphi < 60°$. According to the crystallographic geometry, the vector $\mathbf{P}^*_{011}$ cannot make an angle smaller than 62.8° to N_f if the c axes in the sample are oriented parallel to the film surface because $\mathbf{P}^*_{011}$ makes an angle of 62.8° to b^* axis. The result clearly indicates that the c axes of the crystallites in the sample are almost perfectly oriented parallel to the film surface. We know of no such ordered plane orientation of chain axes, presumably produced only by the effects of crosslinks on crystallization. This highly ordered plane orientation is in accord with the report[28] that uniaxial orientation of the c axis in the crystalline phase of a lightly cross-linked polyethylene that had been highly stretched in the molten state and cooled to room temperature was almost perfect (*i.e.*, the orientation factor was very close to unity).

The orientation of c axes in sample III is less than in sample I as can be seen in Figure 6. But, for simplicity, we will assume that the c axes of the crystallites are oriented parallel to the film plane in addition to the uniaxial orientation of all crystal planes around N_f (random distribution around N_f) in both samples. Then, in so far as this assumption is valid, the remaining freedom in orientation should be only the rotation of crystallites around the c axis. In this case, quantity $(\sin \varphi)I(\varphi)$ will be indicative of the probability density of the rotation, because $(\sin \varphi) \times I(\varphi)d\varphi$ is proportional to the probability that the vector P^*_{hkl} in an arbitrarily chosen crystallite points to the direction between φ and $\varphi + d\varphi$.

Thus, the product $(\sin \varphi)I(\varphi)$ for all crystal axes considered was examined in this sense. Figures 7–10 show the results for the crystal planes (110), (200), (020), and (011), respectively. In each figure, the arrows indicate peak positions when the crystal plane (110) or (200) is preferentially oriented parallel to the film surface. The solid curves are calculated for a distribution of the rotation probability where crystallites are located around c axes with a Gaussian distribution. Here c axes are assumed to locate randomly parallel to the film surface and the peaks for the rotation probability appear when the (110) plane is parallel to the film surface and accordingly the vector $\mathbf{P}^*_{110}$ coinciding with N_f or $\mathbf{P}^*_{\bar{1}10}$ makes an angle of about 67° to it. Here, the plots of $(\sin \varphi)I(\varphi)$ against φ obtained from the X-ray scans for the two samples are roughly nor-

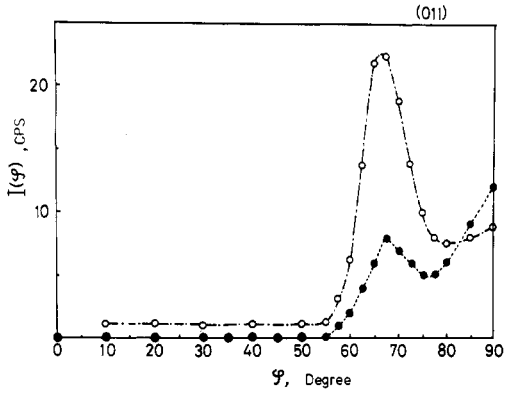

Figure 6. X-ray diffraction scan for the (011) plane. Closed circles: sample I, open circles: sample III in Table I (compression ratio 1:10).

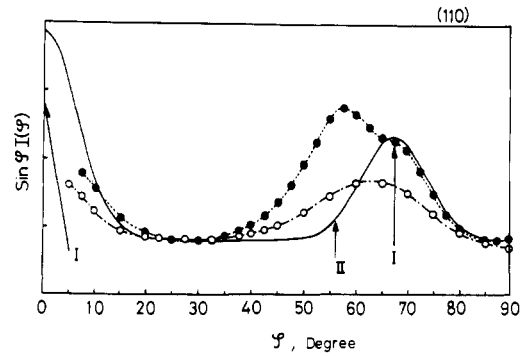

Figure 7. (sin φ)$I(\varphi)$ *vs.* φ for (110): closed circles, sample I; open circles, sample III; solid curve, theoretical curve for the (110) orientation with a Gaussian distribution. Arrow I indicates the peak position for the (110) orientation and II indicates that for the (200) orientation.

malized so that $\int_0^{\pi/2}(\sin\varphi)I(\varphi)d\varphi$ is comparable with the Gaussian distribution.

As can be seen, crystallites in both samples are not rotating around the *c* axis with equal probability but rotating with a preferential probability in special angles. If we examine the experimental data for both samples referring to the hypothetical Gaussian distribution and the arrows, it is clear that crystallites are oriented so that (110) and (200) planes are preferentially oriented parallel to the film surface of both samples. Furthermore, between these two types of orientation, the (200) parallel orientation is shown to be dominant in sample I by enhanced intensities in (sin φ)$I(\varphi)$ at 56° in Figure 7, at 0° in Figure 8 and at 90° in Figures 9 and 10. Thus, it is concluded that the transparent films described in this paper have a very special spatial orientation of crystallites with a parallel orientation of the *c* axis to the film surface and with the (110) and (200) crystal planes preferentially oriented parallel to that surface.

This type of (110) and (200) orientation also has been reported for a biaxially oriented polyethylene[31] and was indicated in the data presented by Sakami and Ida[32] for a cross-linked polyethylene that had been biaxially stretched in the molten state and cooled to room temperature. The origin for these orientations for different samples may be similar. This problem will be discussed in more detail elsewhere. But the authors point out here that, since the (200) parallel orientation is pronounced in sample I and since the molecular chains in this sample

(31) G. C. Adams, *J. Polym. Sci., Part A-2*, 9, 1235 (1971).
(32) H. Sakami and M. Ida, *21st Annu. Meeting Soc. Polym. Chem., Tokyo, 1972, Prepr. No. 1*, 165.

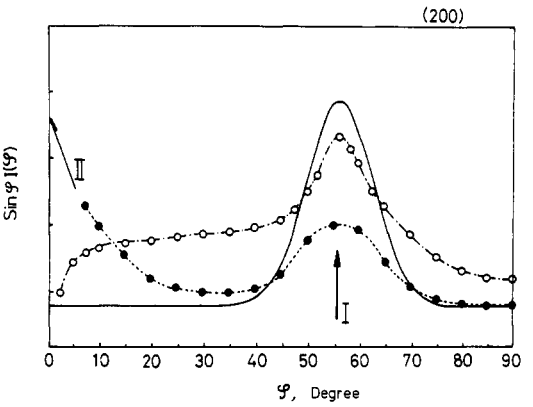

Figure 8. (sin φ)$I(\varphi)$ *vs.* φ for (200). See the legend for Figure 7 for solid curve, arrows, and circles.

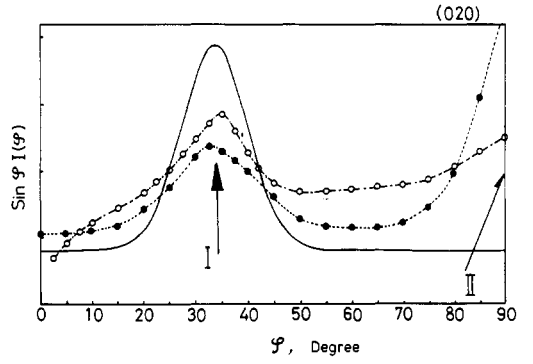

Figure 9. (sin φ)$I(\varphi)$ *vs.* φ for (020). See the legend for Figure 7 for solid curve, arrows, and circles.

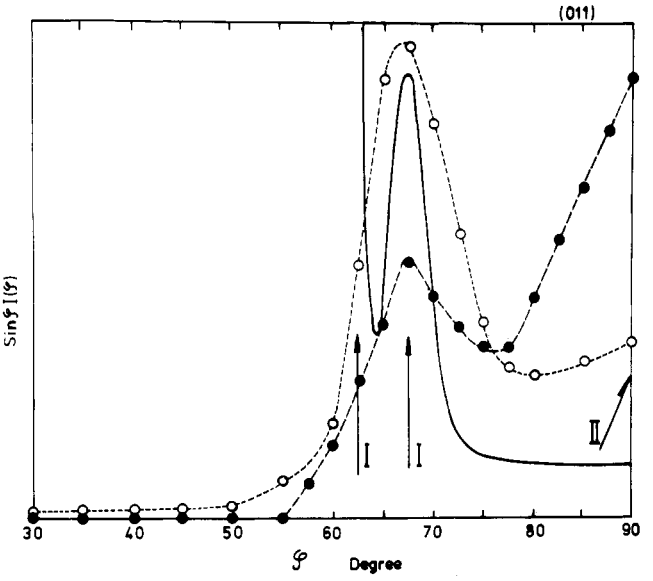

Figure 10. (sin φ)$I(\varphi)$ *vs.* φ for (011). See the legend for Figure 7 for solid curve arrows, and circles.

are thought to be more susceptible to macroscopic deformation in the molten state, this orientation should be unique and characteristic of this mode of crystallization, and probably of more generally oriented crystallizations as well.

The Transparency

In this paper, the authors have repeatedly noted the excellent transparency of the films produced by high compression of the lightly cross-linked samples. However, it is well known that crystalline polyethylene becomes somewhat transparent through plastic flow such as cold draw-

ing. Nevertheless, the transparency of the samples considered here is much superior to that of samples produced through usual procedures.[12] Hence, the origin of the transparency should be considered in a special way.

In general the nontransparency or opaqueness of crystalline polymers is thought to be due to the existence of light-scattering entities such as voids or aggregates of crystallites, whose refractive index is different from that of the amorphous phase. Therefore if the sizes of those entities are smaller than the wavelength of visible light, the samples should become transparent. Wang, Chen, and Kwei[4] supposed that smaller sizes of crystallites accounted for the transparency of the quenched-rolled film made by them. On the other hand, it is pointed out by Stein and Wilson,[33] and by Keijsers, Van Aartsen, and Prins[34] that between the two terms of fluctuation-density and orientation-within crystalline polymers, the latter term usually is primarily responsible for the light scattering in crystalline polyethylene. Based on this fact Desper *et al.*[3] have accounted for the transparency of their samples, made by the capillary-flowing procedure, by assuming a very high orientation of *c* axes and a high degree of crystallinity that could minimize intensity of light scattering. Moreover, based on observations of the light-scattering patterns of samples made by the quenched-rolled technique, Stein and Prud'homme[35] assert that the transparency of such polyethylene films is not primarily related to crystallite size but rather to the type of morphology and to the size of superstructures much bigger than the crystallites themselves.

Thus, the origin of transparency might be different in samples produced by different techniques. However, the excellent transparency of our samples cannot be attributed to either a high degree of crystallinity or to smaller crystallites, since the degree of crystallinity of the samples was unexpectedly low in spite of the high melting temperatures. Also, the low-angle X-ray *d* spacings were either not observed or were larger than 1300 Å.[36] Therefore, we must suppose that the transparency is related to the very special spatial orientation of crystallites in the samples as proposed by Stein and others cited above, and also to the absence of spherulitic structure as concluded by Kawai and Hashimoto[37] from light-scattering data.

Note that the *c* axes of the crystallites in our samples not only orient almost perfectly parallel to the film plane but also that crystal planes (200) or (110) orient predominantly in that direction, and that the low-angle *d* spacings in the direction of the film plane are as large as 1300 Å. Based on these results, we assume that the structure of the samples is composed of aggregations of plate-like crystallites, the planes of which are coincident with either the (110) or (200) crystal planes. It is proposed that major molecular chains cannot exist in the amorphous state between the plane surfaces of the plate-like crystallites but only on their end surfaces, because molecular chains will be mostly parallel to the surface of the crystallites and, hence, will crystallize further. Such a structure accounts for the excellent transparency of our films. Alternatively, light-scattering entities in the samples may be regarded as amorphous phases located in the continuous ordered crystalline phase. Since the amorphous phases are thought to be limited in size, the samples should be transparent.

Conclusions and Summary

Detailed conditons for production of excellent transparent films of linear polyethylene made by irradiation crosslinking have been examined. It is confirmed that the samples have very high melting temperatures and a very stable crystalline phase, but rather low degrees of crystallinity. It is also concluded that the samples have a very special spatial orientation of the crystalline phase. *c* axes are located almost perfectly parallel to the film surface, and the (110) and (200) crystal planes are oriented preferentially parallel to that surface. Furthermore, it is shown that the (200) orientation will be unique and characteristic of this mode of crystallization. Finally, the origin of the excellent transparency is discussed as resulting from a special orientation of the crystalline phase.

Acknowledgment. We express our appreciation to Professors I. Sakurada and W. Tsuji for their useful discussions. The irradiation of the polymer films was performed by the Nuclear Engineering Group in the Faculty of Engineering of Kyoto University and by the Japan Atomic Energy Research Institute with the help of Mr. K. Norizawa and Dr. T. Okada, respectively.

(33) R. S. Stein and P. R. Wilson, *J. Appl. Phys.*, **33**, 1914 (1962).
(34) A. E. M. Keijsers, J. J. van Aartsen, and W. Prins, *J. Appl. Phys.*, **36**, 2874 (1965).
(35) R. S. Stein and R. Prud'homme, *J. Polym. Sci., Part B*, **9**, 595 (1971).
(36) S.-H. Hyon, F. Hamada, and R. Kitamaru, data to be published.
(37) H. Kawai and T. Hashimoto, private communication.